Reactivity of antitumor coinage metal-based N-heterocyclic carbene complexes with cysteine and selenocysteine protein sites.

Iogann Tolbatov[1,2], Tiziano Marzo,[3,4,5] Cecilia Coletti,[2] Diego La Mendola,[3,5] Loriano Storchi,[2] Nazzareno Re,[2] Alessandro Marrone[2]*

[1] Institut de Chimie Moleculaire de l'Université de Bourgogne (ICMUB), UMR CNRS 6302, Université de Bourgogne Franche-Comté(UBFC), avenue Alain Savary 9, 21078 Dijon, France.

[2] Dipartimento di Farmacia, Università "G d'Annunzio" di Chieti-Pescara, Via dei Vestini 31, Chieti, Italy.

[3] Department of Pharmacy, University of Pisa, Via Bonanno Pisano 6, 56126, Pisa, Italy.

[4] CISUP - Centre for Instrumentation Sharing (Centro per l'Integrazione della Strumentazione Scientifica), University of Pisa, Italy.

[5] University Consortium for Research in the Chemistry of Metal ions in Biological Systems (CIRCMSB), Via Celso Ulpiani 27, 70126 Bari, Italy.

KEYWORDS: anticancer, N-heterocyclic carbenes, gold(I) complexes, silver(I) complexes, copper(I) complexes, DFT calculations, proteins

ABSTRACT

The reaction of the antitumor M(I)-bis-N-heterocyclic carbene complexes, M=Cu, Ag, and Au, with their potential protein binding sites, i.e. cysteine and selenocysteine, was investigated by means of density functional theory approaches. Capped cysteine and selenocysteine were employed to better model the corresponding residues environment within peptide structures. By assuming the neutral or deprotonated form of the side chains of these amino acids and by considering the possible assistance of an external proton donor such as an adjacent acidic residue or the acidic component of the surrounding buffer environment, we devised five possible routes leading to the binding of the investigated M(I)-NHC scaffolds to these protein sites, reflecting their different location in the protein structure and exposure to the bulk. The targeting of either cysteine or selenocysteine in their neutral forms is a kinetically unfavored process, expected to be quite slow if observable at all physiological temperature. On the other hand, the reaction with the deprotonated forms is much more favored, even though an external proton source is required to assist the protonation of the leaving carbene. Our calculations also show that all coinage metals are characterized by a similar reactivity toward the binding of cysteine and selenocysteine sites, although the Au(I) complex has significantly higher reaction and activation free energies compared to Cu(I) and Ag(I).

Introduction

The catalytic properties of metal complexes with N-heterocyclic carbene (NHC) ligands are the main reason behind their ubiquitous use [1, 2]. While NHC ligands are rather unstable in protic solvent, the coordination via a strong carbon-to-metal σ donation of the sp^2 lone pair induces a marked stabilization of their metal complexes, even in aqueous solutions [3-5]. On the other hand, their exceptional flexibility, in terms of their facile decoration with different chemical functions, is an attractive feature for the development of drugs, by allowing a tight control of their biological properties and selectivity for specific targets. For this reason, a plethora of platinum, palladium, ruthenium, rhodium, nickel, iridium, gold, silver, and copper carbenes have been studied [6-13]. Moreover, there is recent evidence that metal NHC complexes can be utilized to design highly efficient metal-based drugs with potential applications in anticancer and antibacterial therapies [6, 14].

In particular, gold complexes with N-heterocyclic carbene (HNC) ligands are an auspicious class of anticancer metallodrugs which demonstrate powerful cytotoxic effects *in vitro* and *in vivo* [15-18]. Several mechanisms of action have been proposed for cell apoptosis induced by Au(I): direct DNA damage, topoisomerase inhibition, or mitochondrial damage including thioredoxin reductase (TrxR) inhibition [19, 20]. Among them, this latter mechanism seems to play a central role in the pharmacology of gold complexes as gold displays a high affinity to thiol and selenol groups. TrxR isoforms are predominantly detected in the cytoplasm and mitochondria, their main role being the maintenance of the redox balance of the cell by means of participating of an enzymatic cascade deputed at the reduction of hydrogen peroxide. Furthermore, it was noted that the TrxR systems are overexpressed in some types of cancer [21, 22]. Additionally, the Au(I) fragments typically derived from the gold-based complexes were highlighted as potent inhibitors of the closely related

Se-free enzyme glutathione reductase (GR), owing to the high thiol reactivity toward gold, as was recently shown in the crystal structure of GR inhibited by a gold(I) complex that displays Au(I) bound to the active site Cys thiols with nearly linear S-Au-S coordination [10, 23, 24]. These NHC complexes mainly belong to two classes (i) mono-carbene adducts of metals salts that also bind a labile ligand X, such as in (NHC) MX, usually X = halide, with the X ligand expected to be readily substituted under physiological conditions and susceptible to substitution by intracellular thiols; (ii) ionic biscarbene complexes $[M(NHC)_2]^+X^-$, which can bind to the thiols or selenols targets only after carbene dissociation.

Reports on silver carbenes anticancer activity are fewer than on gold-based ones [25-30]. Notwithstanding this scarcity, recently, their antitumor activity was found to be analogous or even greater than in gold carbenes [30, 31]. Recent studies have shown a strong inhibition of TrxR activity for Ag(I) NHC complexes, thus suggesting that this could be a viable mechanism of action also for this class of silver compounds [32-34]. A recent study by some of the authors reported on the complex bis(1-(anthracen-9-ylmethyl)-3-ethylimidazol-2-ylidene) silver chloride ($[Ag(EIA)_2]Cl$) which shows a high anticancer potency in SH-SY5Y neuroblastoma cancer cells likely relying on the TRxR inhibition. Indeed, ($[Ag(EIA)_2]Cl$ was able to bind the C-terminal dodecapeptide hTrxR(488–499) reproducing the active site of thioredoxin reductase and inhibiting the enzymatic activity. Furthermore, anthracene functionalized silver carbenes were found to inhibit TrxR [35] and their use includes the possibility of imaging upon administration to cells; yet their DNA binding has only been marginally explored [36]. Moreover, it was noted that silver compounds are capable to targeting non-genomic targets such as mitochondria and proteins [30,31, 37, 38].

In the last years, copper-based carbene complexes have also attracted growing attention in the field for their potential application in medicine. Specifically, several Cu-NHC complexes have been synthesized and tested for application as anticancer, antiparasitic and antimicrobial agents with some encouraging results [39, 40] The mechanism of activation of Cu(I) NHC complexes is even less clear, since copper is an essential element in human body involved in many biological pathways, and several possible mechanisms have been proposed including the interconversion to Cu(II) species in oxidation–reduction cycles promoting DNA breaking or generating reactive oxygen species (ROS) that overwhelm cellular antioxidant defenses to produce oxidative damages in the cytoplasm, mitochondria, and DNA [41, 42]. However, the analogy with isostructural silver(I) and gold(I) compounds suggests that TrxR inhibition is also a viable process for copper NHC complexes as supported by recent studies showing that copper(I) compounds as well as silver(I), and gold(I) analogs were able to strongly decrease TrxR activity [43].

In the last 20 years, several theoretical studies have elucidated the fundamental reasons behind the stability of free NHCs and the metal-NHC bond [44-47]. Calculations on the CCSD(T) level of theory indicated a trend of Au>Cu>Ag for the dissociation energies of coinage metal-NHC bonds [45]. These metal-NHC bonds are dominantly electrostatic in nature with minor covalent interactions. The covalent interaction is largely σ-bonding [46]. DFT calculations indeed suggest that NHCs are stronger σ-donors and weaker π-acceptors than phosphine ligands [46]. More recently a few theoretical studies [48-50] investigated the antitumor activity of Au(I) N-heterocyclic carbene complexes focusing on their binding to cysteine or selenocysteine nucleophiles to model the GR or TrxR enzyme binding site, and analizing in detail the binding mechanism and the corresponding energy profiles. In a recent study, we investigated a wide range of possible pathways for gold bis-N-heterocyclic carbenes binding to cysteine and selenocysteine

residues of proteins surfaces [48]. DFT calculations have shown that in the case of carbene substitution in the Au(I)-NHC complexes $[(Me_2Im)_2Au]^+$ by cysteine and selenocysteine, a crucial role is played by the proton transfer from thiol or selenol groups or by an external proton source, like the acidic component of a phosphate buffer, to the leaving carbene moiety. To our knowledge, no computational studies on the reactivity of Ag(I)- and Cu(I)-NHC complexes with cysteine and selenocysteine were performed, despite Ag(I)-NHC recently being confirmed a potential antitumoral agent [25-30]. Indeed, a deeper insight into the detailed mechanism of action of these coinage metal complexes would be very important in order to compare their mechanisms of action *in vivo*, thus serving for the design of new and more potent coinage metal based anticancer drugs.

In this study, the reaction of coinage metals bis-NHC complexes with cysteine (Cys) and selenocysteine (Sec) as models of the GR or TrxR enzyme binding site were investigated by means of density functional theory approaches. By using the capped version of both Cys and Sec, we model the corresponding residues environment within the peptide structure and alleviate the potential artifacts connected to the use of the ionized form of N and C terminals, typical of the free amino acids. Furthermore, the use of the caps avoids possible problems due to the preference of these amino acids towards their zwitterionic form. Following the same approach of ref. [48], we consider five different routes for the exchange of the NHC ligand by either the thiol or selenol side chain of Cys or Sec, respectively. These five reaction models allow to get an insight on the influence of the protein environment on the binding of M(I)-NHC scaffolds. The results also highlight the importance of the ionization state of Cys and Sec side chains and of the chemical environment assisting the substitution of NHC ligands at coinage metal centers, thus paving the structural basis to the binding of M-NHC scaffolds to either neutral or deprotonated thiol and selenol groups.

Computational Details

All calculations were performed with the Gaussian 09 A.02 [51] quantum chemistry package.

Geometrical optimizations were carried out in solution by using B3LYP in combination with the LANL2DZ basis set for metals [52] and the 6-31+G* basis set for other atoms [53-55]. Solvation energies were also obtained from the above calculations. Frequency calculations were performed to verify the correct nature of the stationary points and to estimate zero-point energy (ZPE) and thermal corrections to thermodynamic properties. Intrinsic reaction coordinate (IRC) calculations were employed to check the connection of the identified transition state for each considered reaction step with reactant and product minima.

Single-point electronic energy calculations on the resulting geometries were then performed by using the range-corrected functional ωB97X with the basis sets LANL08(f) [52, 56] for the metals and 6-311++G** basis sets for the other elements [53, 57].

Indeed, DFT gives a good description of geometries and reaction profiles for transition-metal-containing compounds [57-61] including Au-, Ag- and Cu-based anticancer compounds [48,49, 62-65]. B3LYP is known to yield accurate geometrical structures [49, 67, 68], and ωB97X [69] has been reported to reach a high accuracy in the calculation of electronic energies [70,71]. The C-PCM continuum solvent method was used to describe the solvation [72]. It has recently been shown to give considerably smaller errors than those for other continuum models for aqueous solvation free energies for neutrals and ions [73].

Results and Discussion

The molecular structure of M(I)-bis-carbene complexes such as $[(Me_2Im)_2M]^+$ (M = Au, Ag, Cu) is characterized by the high stability of the M–C bonds, and by their rotational asset that locates the N-bound methyl groups in proximity to the metal center. These two structural elements play a crucial role in the control of the reactivity of the considered metal complexes with their final endogenous targets. A preliminary investigation on the isolated Au(I)-, Ag(I)-, and Cu(I)-NHC complexes $[(Me_2Im)_2M]^+$ (M = Au, Ag, Cu) has shown that at the selected level of theory the minimized structure matches the crystallographic data for $[(Me_2Im)_2M]^+$ accurately with bond distances within 0.04, 0.04, and 0.05 Å for Au, Ag, and Cu, respectively, thus indicating that the B3LYP functional provides a good description of these molecular structures (see Figure 1 and Table 1).

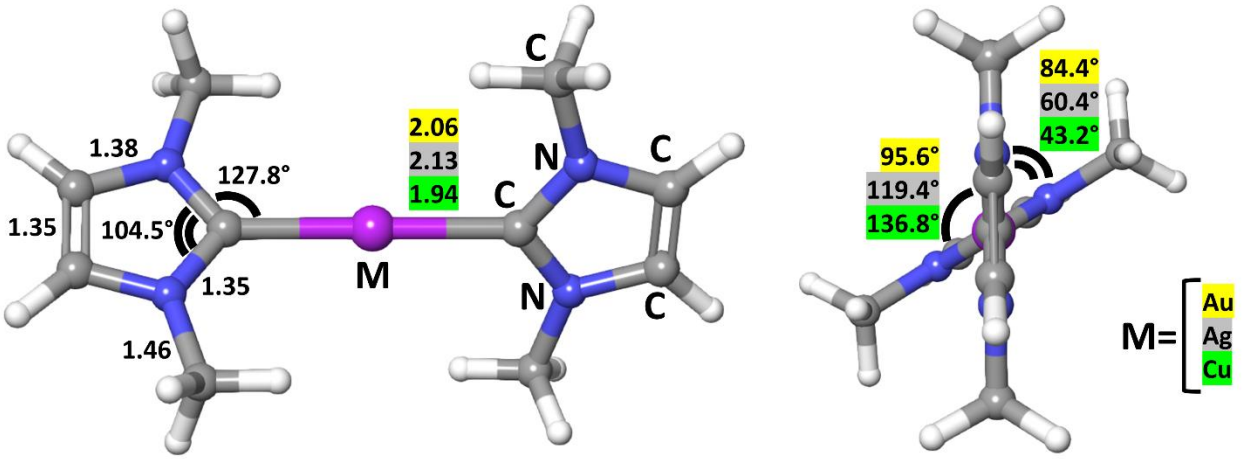

Figure 1. Calculated geometrical structure of Au(I)-NHC complex. Distances are in angstroms, angles in degrees.

Table 1. Comparison of calculated and experimental Metal-$C_{carbene}$(NHC) bonds and minimal metal···hydrogen (N-methyl) distances in Angstrom.

Metal	M–C distance		M···H minimal distance	
	calc	exp	Calc	exp
Au	2.06	2.05 [35]	2.86	3.12 [35]
		2.02 [74]		2.95 [74]
Ag	2.13	2.09, 2.10 [28]	2.88	3.07 [28]
		2.09 [35]		3.15 [35]
		2.10, 2.12 [75]		3.06 [75]
		2.08, 2.16 [76]		2.92, 3.04 [76]
Cu	1.94	1.89 [77]	2.78	3.07 [77]

Calculated and experimental data show the same trend of M–C distances, i.e. Cu < Au < Ag, which is consistent to the valence shell radius of each M(I) center. As expected, a similar trend was detected in the M···H minimal distances, although both calculated and experimental values, in the 2.75-2.90 and 2.90-3.15 Å ranges, respectively, rule out any possibility for the formation of agostic interactions between the metal center and the hydrogens of N-methyl groups. Thus, the capability of the M(I)-NHC complexes to react in ligand exchange reactions is expected to be mainly affected by the strength of the M–C bond, while the steric influence of the N-methyl groups is marginal.

DFT calculations were carried out on the thermodynamics of the exchange of one carbene ligand by an incoming capped cysteine or selenocysteine molecule or by their corresponding anion. Five different possible reaction paths were taken into account: (1) the cysteine thiol or selenocysteine

selenol group replaces the NHC ligand keeping its proton, (2) the thiol or selenol proton is transferred to the leaving carbene ligand in the course of the substitution reaction, (3) a proton from the acidic component of a phosphate buffer is transferred to the leaving carbene ligand in the course of the substitution reaction, (4) the anionic thiolate or selenolate group replaces the NHC ligand, and (5) the deprotonated thiolate or selenolate nucleophile replaces the NHC ligand, which is stabilized by a proton transfer from the acidic component of the phosphate buffer while detaching from the metal center (Table 2).

Table 2. Gibbs free energies for reactions (1)-(5). Reported values are in kcal/mol.

	Reactants		Products		Cys			Sec		
	M-bis-NHC	nucleophile	bound M-NHC	leaving carbene	Au	Ag	Cu	Au	Ag	Cu
(1)	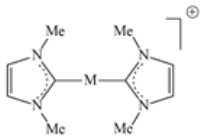		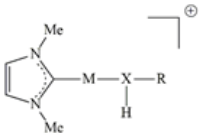	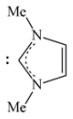	34.9	24.4	25.6	33.2	23.9	21.8
(2)	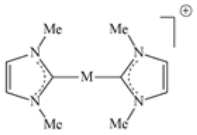		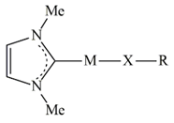	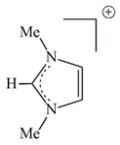	-6.1	-10.6	-10.4	-10.7	-14.9	-13.0
(3)	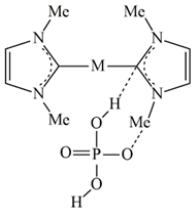		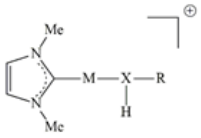	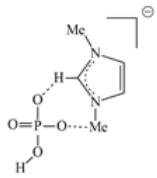	26.0	15.6	19.1	24.2	15.1	15.2
(4)	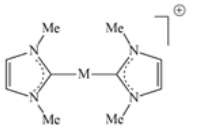		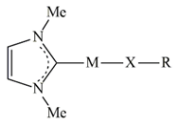	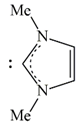	9.6	5.1	5.4	11.9	7.7	9.6
(5)	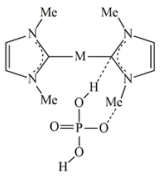		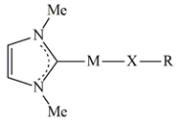	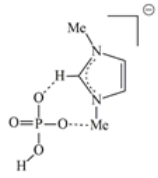	0.6	-3.7	-1.2	2.9	-1.1	3.0

As expected, pathway (1), whereby the reaction of $[(Me_2Im)_2M]^+$ with the neutral amino acid occurs without proton transfer, is thermodynamically highly unfavorable with values of 33.2, 23.9, and 21.8 kcal/mol for selenocysteine, and even higher for cysteine, for Au, Ag, and Cu, respectively. On the other hand, pathway (2), including the proton transfer (PT) from the incoming neutral amino acid to the leaving carbene, greatly stabilizes the latter and the reaction free energies drop down to -6.1, -10.6, -10.4 kcal/mol for Au, Ag, and Cu, respectively, in case of reaction with cysteine, whereas the corresponding values for the reactions with selenocysteine are, in the same order, -10.7, -14.9, and -13.0 kcal/mol. These results indicate the crucial role played by the protonation of the leaving carbene to make its substitution thermodynamically feasible for all considered metals. In principle, protons could be delivered by an external source, such as a water molecule, an acidic group of an adjacent residue or the acidic component of the surrounding buffer environment. Among them, we explored the last possibility, considering the ubiquitous presence of phosphate buffer in the cytosol of all cells, with the dihydrogen phosphate anion $H_2PO_4^-$ as acidic component. This is also one of the most common buffers in the *in vitro* reactions between gold complexes and enzymes, peptides or simple amino acids. As expected, the buffer assistance (reaction (3)) promoting the PT from the phosphate to the leaving carbene lowers the reaction energy by ~10 kcal/mol with respect to the corresponding values from reaction (1), yielding 24.2, 15.1, and 15.2 kcal/mol for the reaction of Sec with Au, Ag, and Cu, respectively. Such decrease however is not enough to produce a significant thermodynamic enhancement of the reaction between M(I)-NHC complexes and either Cys or Sec side chains, suggesting that deprotonation of the target S–H or Se–H groups, known to strongly increase their nucleophilicity, is also required. Moreover, at pH 7.4 – typical in physiological conditions – the fraction of deprotonated Cys and Sec equals 5% and 98%, respectively (calculated by the pKa values of 8.3 for Cys and 5.2 for Sec)

so that we also consider pathways (4) and (5) with deprotonated amino acids. Despite the expected enhanced nucleophilicity of deprotonated amino acids, the free energies for pathway (4) without any proton transfer to the leaving carbene remain positive for all the studied complexes: 9.6, 5.1, 5.4 kcal/mol for the reaction with cysteine of Au, Ag, and Cu metal complexes, respectively, and, in the same order, 11.9, 7.7, 9.6 kcal/mol for the reaction with selenocysteine. If the attack by the deprotonated Cys^- and Sec^- species is instead assisted by PT from the phosphate buffer to the leaving carbene, as in pathway (5), the reaction free energies are further decreased becoming exergonic in most cases: 0.6, -3.7, -1.2 kcal/mol for the reaction of Au, Ag, and Cu complexes, respectively, with cysteine; and 2.9, -3.1, 3.0 kcal/mol for the corresponding reaction with selenocysteine.

These results indicate that only pathways (2) and (5) are thermodynamically allowed, highlighting the importance of the concomitant proton transfer to the leaving carbene and Cys/Sec deprotonation. We thus focused on the kinetics of pathways (2) and (5) alone, that were investigated through supermolecular models by considering that both reagents and products can form non-covalent adducts prior – reactant adduct (RA) – and after – product adduct (PA) – the ligand substitution takes place. Although the hypothesized formation of RA and PA intermediates between the metal complexes and the Cys or Sec models could be considered as merely artifacts of the adopted supermolecular model, when the real protein targets are considered, these metal complexes might non-covalently interact with the protein environment while approaching their binding sites. As remarked in Ref. [78], the free energy for the formation of the RA adduct from R represents an estimate of the energy cost required to approach the metal center in proximity with the final covalent binding site of the model capped amino acids; such energy cost may be compensated by the non-covalent interactions of the metal complex with the real protein

environment. We thus take into account two reference states for the calculation of the activation free energy: on one hand, the free energy for the RA→TS step estimates the barrier for the metal-protein binding by assuming the metal scaffold already in proximity of its final binding sites, i.e. Cys or Sec residues, on the other hand, the free energy for the R→TS step estimates the overall barrier for the formation of the metal-protein adduct and includes the energy cost for moving the metal complex from the bulk to the protein site, the latter value might be overestimated by the use of model amino acids and of a supermolecular approach. In this way RA→TS can be considered as a lower and R→TS as an upper limit to the activation energy for carbene substitution. Analogously, the PA→P step can be assumed to model the detachment of the released NHC from the metal-binding site of the protein to the bulk. It must be remarked that the reported R→RA or PA→P free energy values are thus only upper estimates of the free energy costs/gains involved in the M(I)-NHC approach to protein/free carbene release, respectively.

Table 3. Activation free energies for reactions (2) and (5). All values are in kcal/mol.

Reaction	M	AA	R→TS	RA→TS
(2)	Au	CysH	40.9	32.6
	Ag		29.3	20.3
	Cu		31.7	24.9
	Au	SecH	37.6	30.3
	Ag		28.4	20.3
	Cu		31.3	24.0
(5)	Au	Cys-	18.0	13.4
	Ag		6.8	3.3
	Cu		7.8	3.8
	Au	Sec-	19.8	12.7
	Ag		12.7	5.1
	Cu		13.6	5.6

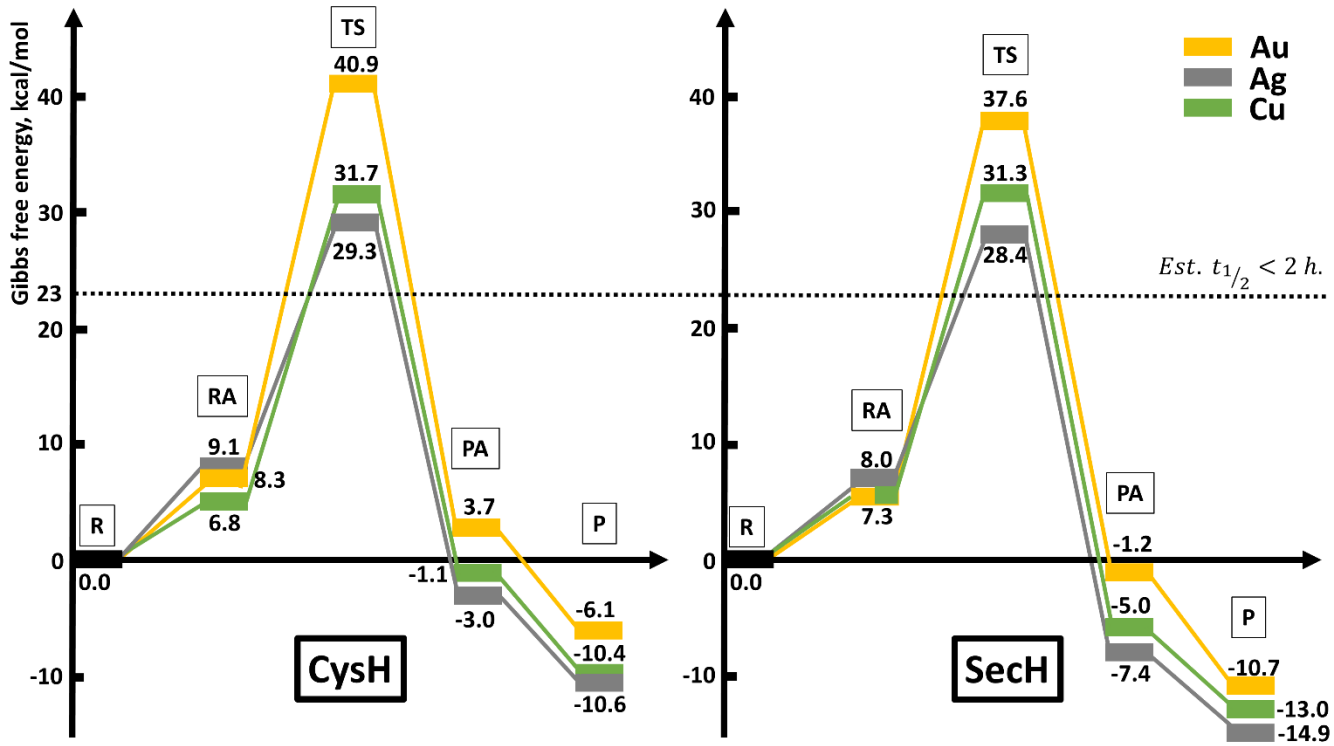

Figure 2. Free energy profiles for pathway (2) of M(I)-NHC complexes with neutral Cys and Sec. The dashed line at 23 kcal/mol represents the barrier corresponding to an estimated half-time of 2 h ca. All values in kcal/mol.

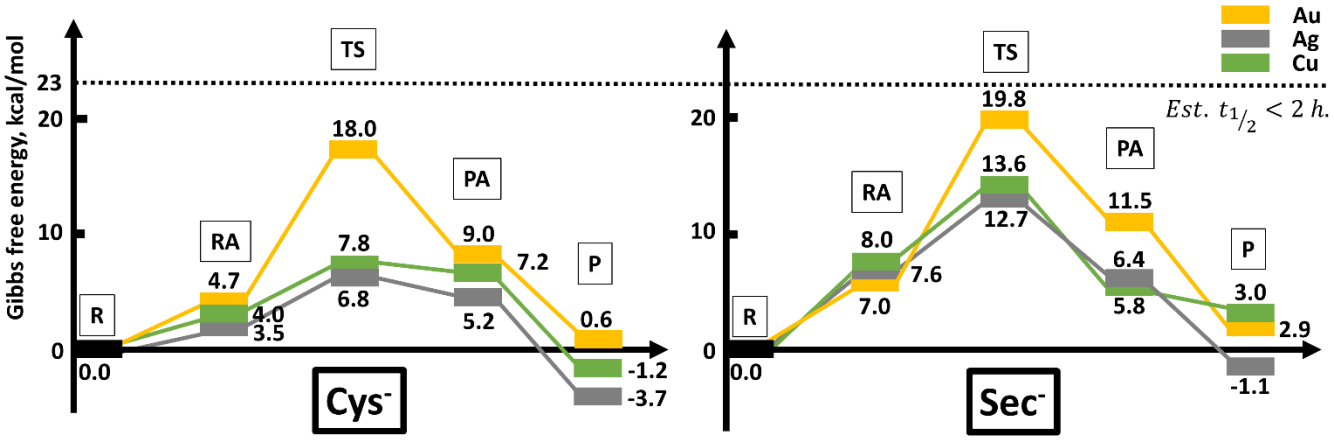

Figure 3. Free energy profiles for pathway (5) of M(I)-NHC complexes with deprotonated Cys and Sec. The dashed line at 23 kcal/mol represents the barrier corresponding to an estimated half-time of 2 h ca. All values in kcal/mol.

For pathway (2) we calculated upper limits to the activation free energy of NHC substitution (R→TS) in the range 31-41 kcal/mol for Au and Cu, and 28-29 kcal/mol for Ag (Table 3, Figure 2) suggesting that these reactions are kinetically unfeasible (Au, Cu) or unlikely (Ag) at room or physiological temperature. On the other hand, the calculated lower limits to activation free energy (RA→TS) are in the range 20-25 kcal/mol for Ag and Cu complexes but 30-33 kcal/mol for Au(I), thus indicating that the binding to neutral thiol or selenol groups is kinetically feasible for Ag(I) and Cu(I) but not for Au(I) complexes. Pathway (5), on the other hand, yields low R→TS activation free energy upper limits for the reactions of Au, Ag, and Cu complexes with deprotonated Cys, 18.0, 6.9 and 7.8 kcal/mol respectively, and with deprotonated Sec, 19.8, 12.7 and 13.6 kcal/mol, and even lower RA→TS estimates (Table 3, Figure 3). Therefore, all coinage metal complexes disclose a high reactivity for thiolate and selenolate groups with buffer assisted proton transfer through pathway (5). The low activation free energies calculated for pathway (5) indicate that the binding of $[(Me_2Im)_2M]^+$ metal complexes to deprotonated amino acids is under thermodynamic control, whereas the metal binding at the corresponding neutral aminoacids (reaction (2)) is under kinetic control (Table 3).

The calculated transition state structures for pathway (2) are reported in Figure 4. Typically, the entering neutral nucleophile approaches the metal center, whereas the NHC group moves further; an approximatively planar trigonal geometry is observed, with an acute leaving ligand–metal–entering ligand angle of 70-80°. Moreover, the relatively short M-S/Se and long M-C bond lengths indicate rather late transition states, consistently with the T-shape distorted trigonal geometry. Such a transition state structure is consistent with the data in literature, indicating that gold(I) linear complexes undergo ligand substitution reactions via an associative interchange mechanism, passing through a tricoordinate transition state [47, 48]. As already detected in the optimized

structure of these M(I)-NHC complexes, the presence of various metals in these transition states reflects their different valence shell radius. Hence, shorter M–C and M–S/Se bonds are formed by Au(I) and Cu(I) metal centers. On the other hand, the metal effect on the lateness of these structures is displayed by the lengths of the incoming M – C and C – H bonds that indicate an Au(I)>Ag(I)>Cu(I) trend (Figure 4).

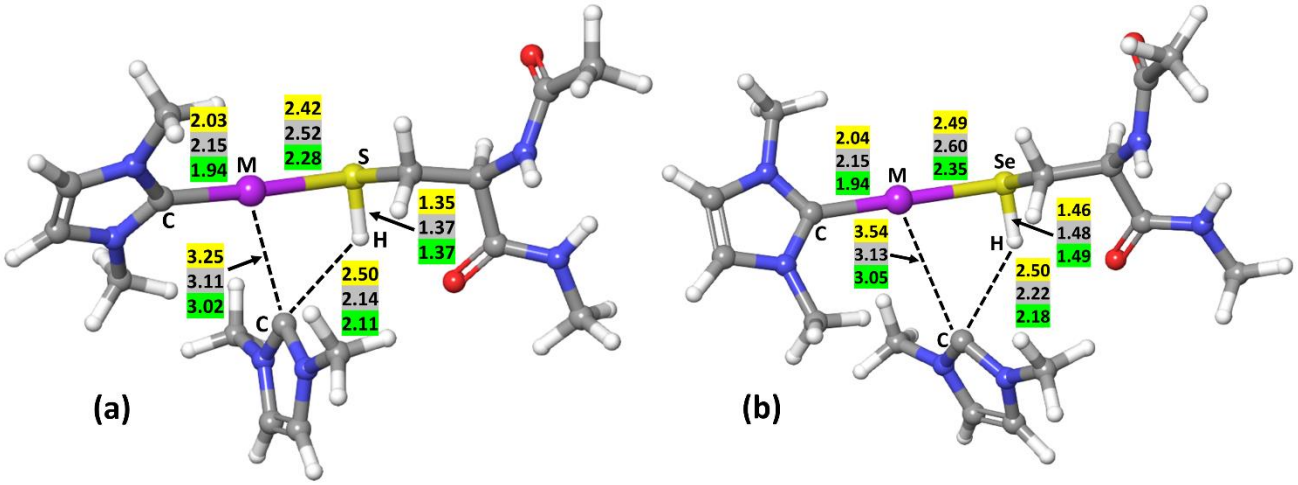

Figure 4. Transition state structures for pathway (2) with neutral Cys (a) and neutral Sec (b). The distances are highlighted with different colors for different metals: gold (yellow), silver (gray), copper (green). Distances are in angstroms.

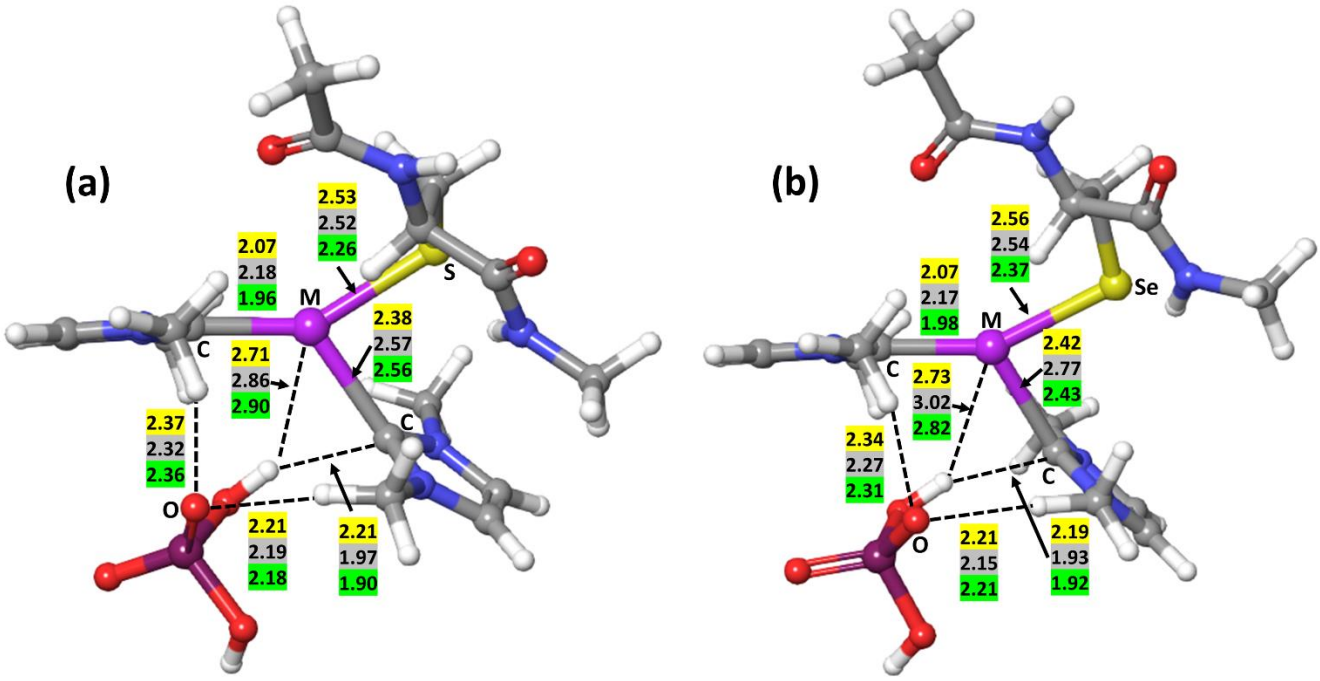

Figure 5. Transition state structures for the buffer-assisted pathway (5) with deprotonated Cys (a) and deprotonated Sec (b). The distances are highlighted with different colors for different metals: gold (yellow), silver (gray), copper (green). Distances are in angstroms.

The calculated transition state geometries for pathway (5) are reported in Figure 5. These structures are consistent with earlier transition states compared to reaction (2), as reflected by the significantly shorter M–C distances, by almost 1 Å. The approximatively planar trigonal geometries, with an acute leaving ligand–metal–entering ligand angle of 70-80°, C–M–C angles larger than 90°, indicate an earlier character of these TS structures. The assistance of the phosphate buffer is realized by the interaction of the hydrogen atom of a hydroxyl group of the phosphate anion with the carbon of the leaving carbene, and by the interaction of the same hydrogen with the metal center. The oxygen of phosphate also forms weak interactions with the hydrogen atoms of the methyl groups on both carbenes (Figure 5).

Conclusions and further remarks

We have performed a detailed theoretical study on the mechanism of carbene ligand substitution by capped cysteine and selenocysteine molecules, as models of the corresponding protein side chains, in Au(I), Ag(I), and Cu(I) bis-N-heterocyclic carbene complexes. Computational studies indeed offer a valuable tool to predict, support and validate the experimental results. Moreover, the selenocysteine of thioredoxin reductases (TrxR) is the preferential binding site of many antitumor metallodrugs and has recently been shown to be targeted by Au(I)-, Ag(I)- and possibly Cu(I)-NHCs.

Accordingly, we have studied several possible pathways allowing for the protonation of the leaving carbene moiety by the neutral thiol/selenol group or by an acidic buffer component from the surrounding environment, to model the different chemical backgrounds where these ligand exchange processes may occur. Indeed, the protonation of the leaving carbene is a thermodynamic caveat which has to be ensured by either the protein or the bulk. The analysis of reaction free energies indicates that neutral Cys and Sec, although less reactive in comparison with their deprotonated forms, can be targeted by the considered biscarbene complexes but only for Ag(I) and, to a lesser extent, for Cu(I). The reaction with deprotonated Cys or Sec is kinetically favored but requires the assistance of an external proton source such as a buffer to accomplish the proton transfer to the leaving carbene.

The present results indicate that the buffer assisted reaction of the $[(Me_2Im)_2M]^+$ metal complexes with the deprotonated Cys and Sec is fast and under thermodynamic control, whereas their reaction with neutral Cys and Sec, viable only for Ag(I) and Cu(I), is relatively slow and under kinetic control, and more affected by the interaction of the metal scaffold with the protein environment. In both cases, the analyzed coinage metal complexes disclose both kinetic and

thermodynamic preference in the order Ag(I) > Cu(I) > Au(I) clearly indicating that binding to the thiol or selenol targets of Ag(I) complexes are both kinetically and thermodynamically favored. This result agrees with experimental evidence showing that, among the NHC complexes of group 11 metals, silver NHC complexes are known for their lability and indeed have been used as NHC transfer reagents for the synthesis of NHC complexes of other metals [79]. As a result, (NHC)Ag compounds may lose their structural integrity under physiological conditions precluding quantitative structure–activity relationships.

Indeed, notwithstanding the higher *in vitro* inhibition of TrxR by Ag(I) than Au(I) NHC complexes, the antitumor activity does not always follow the same trend [80], probably because of the higher lability of Ag(I) complexes hindering them to reach their targets *in vivo*. Therefore, the relative cytotoxicity of Ag(I) and Au(I) NHC complexes is determined by a trade-off between the higher reactivity of silver compounds towards the selenol targets and the higher ability of gold complexes to reach them. The reactivity of copper compounds is in between, thus supporting TrxR inhibition as a viable mechanism of action also for the lightest coinage metal complexes.

Work is in progress to further rationalize the behavior of the different coinage metal complexes according to the different chemically meaningful contributions to the bond energy [81,82].

Supporting Information. The following files are available free of charge: A word file containing the optimized molecular structures of minima and transition states of the mechanisms described in the paper in Cartesian atomic coordinates in standard .xyz file format.

Corresponding Author

Cecilia Coletti, Dipartimento di Farmacia, Università "G d'Annunzio" di Chieti-Pescara, Via dei Vestini 31, Chieti, Italy. E-mail: ccoletti@unich.it

Author Contributions

The manuscript was written through contributions of all authors. All authors have given approval to the final version of the manuscript.

Acknowledgements

TM and DM thank Beneficentia Stiftung (Vaduz) BEN2019/48 for the financial support. This work was also supported by the University of Pisa under the Rating Ateneo 2020 and "PRA – Progetti di Ricerca di Ateneo" Institutional Research Grants – Project no. PRA_2020_58 "Agenti innovative e nanosistemi per target molecolari nell'ambito dell'oncologia di precisione" to TM and DM.

REFERENCES

[1] Herrmann, W.A. N-heterocyclic carbenes: A new concept in organometallic catalysis. *Angew. Chem. Int. Ed*. **2002**, *41*, 1290-1309.

[2] Hopkinson, M.N.; Richter, C.; Schedler, M.; Glorius, F. An overview of N-heterocyclic carbenes. *Nature* **2014**, *510*, 485-496.

[3] Gandin, V.; Pellei, M.; Marinelli, M.; Marzano, C.; Dolmella, A.; Giorgetti, M.; Santini, C. Synthesis and in vitro antitumor activity of water-soluble sulfonate-and ester-functionalized silver (I) N-heterocyclic carbene complexes. *J. Inorg. Biochem*. **2013**, *129*, 135-144.

[4] Hung, F.F.; To, W.P.; Zhang, J.J.; Ma, C.; Wong, W.Y.; Che, C.M. Water-soluble luminescent cyclometalated gold (III) complexes with cis-chelating bis (N-heterocyclic carbene) ligands: Synthesis and photophysical properties. *Chem. - A Eur. J.* **2014**, *20*, 8604-8614.

[5] Luo, F.T.; Lo, H.K. Short synthesis of bis-NHC-Pd catalyst derived from caffeine and its applications to Suzuki, Heck, and Sonogashira reactions in aqueous solution. *J. Organomet. Chem.* **2011**, *696*, 1262-1265.

[6] Ott, I., 2017. Medicinal chemistry of metal N-heterocyclic carbene (NHC) complexes. In Inorganic and Organometallic Transition Metal Complexes with Biological Molecules and Living Cells (pp. 147-179). Academic Press.

[7] Mercs, L.; Albrecht, M. Beyond catalysis: N-heterocyclic carbene complexes as components for medicinal, luminescent, and functional materials applications. *Chem. Soc. Rev.* **2010**, *39*, 1903-1912.

[8] Marinelli, M.; Santini, C.; Pellei, M. Recent advances in medicinal applications of coinage-metal (Cu and Ag) N-heterocyclic carbene complexes. *Curr. Top. Med. Chem.* **2016**, *16,* 2995-3017.

[9] Mora, M.; Gimeno, M.C.; Visbal, R. Recent advances in gold–NHC complexes with biological properties. *Chem. Soc. Rev*. **2019**, *48*, 447-462.

[10] Oehninger, L.; Rubbiani, R.; Ott, I. N-Heterocyclic carbene metal complexes in medicinal chemistry. *Dalt. Trans*. **2013**, *42*, 3269-3284.

[11] Medici, S.; Peana, M.; Crisponi, G.; Nurchi, V.M.; Lachowicz, J.I.; Remelli, M.; Zoroddu, M.A. Silver coordination compounds: A new horizon in medicine. *Coord. Chem. Rev.* **2016**, *327*, 349-359.

[12] Streciwilk, W.; Terenzi, A.; Cheng, X.; Hager, L.; Dabiri, Y.; Prochnow, P.; Bandow, J.E.; Wölfl, S.; Keppler, B.K.; Ott, I. Fluorescent organometallic rhodium (I) and ruthenium (II) metallodrugs with 4-ethylthio-1, 8-naphthalimide ligands: Antiproliferative effects, cellular uptake and DNA-interaction. *Eur. J. Med. Chem*. **2018**, *156*, 148-161.

[13] Zhang, J.J.; Muenzner, J.K.; Abu El Maaty, M.A.; Karge, B.; Schobert, R.; Wölfl, S.; Ott, I. A multi-target caffeine derived rhodium (I) N-heterocyclic carbene complex: evaluation of the mechanism of action. *Dalton Trans*. **2016**, *45*, 13161-13168.

[14] Liu, W.; Gust, R. Update on metal N-heterocyclic carbene complexes as potential anti-tumor metallodrugs. *Coord. Chem. Rev*. **2016**, *329,* 191-213.

[15] Casini, A.; Suns, R.W.Y.; Ott I. Medicinal chemistry of gold anticancer metallodrugs. In Sigel, A.; Sigel, H.; Freisinger, E.; Sigel, R.K.O. (Eds) Metallo-drugs: Development and action of anticancer agents. Basel, 2018: 199-217.

[16] Al-Majid, A.M.; Yousuf, S.; Choudhary, M.I.; Nahra, F.; Nolan, S.P. Gold-NHC complexes as potent bioactive compounds. *ChemistrySelect* **2016**, *1*, 76-80.

[17] Hickey, J.L.; Ruhayel, R.A.; Barnard, P.J.; Baker, M.V.; Berners-Price, S.J.; Filipovska, A. Mitochondria-targeted chemotherapeutics: The rational design of gold (I) N-heterocyclic carbene complexes that are selectively toxic to cancer cells and target protein selenols in preference to thiols. *J. Am. Chem. Soc.* **2008**, *130*, 12570-12571.

[18] Oberkofler, J.; Aikman, B.; Bonsignore, R., Pöthig; A., Platts, J.; Casini, A. and Kühn, F.E. Exploring the Reactivity and Biological Effects of Heteroleptic N-Heterocyclic Carbene Gold(I)-Alkynyl Complexes. *Eur. J. Inorg. Chem*., **2020**, *2020*, 1040-1051.

[19] Magherini, F.; Fiaschi, T.; Valocchia, E.; Becatti, M.; Pratesi, A.; Marzo, T.; Massai, L.; Gabbiani, C.; Landini, I.; Nobili, S.; Mini, E.; Messori, L.; Modesti, A.; Gamberi, T. Antiproliferative effects of two gold (I)-N-heterocyclic carbene complexes in A2780 human ovarian cancer cells: a comparative proteomic study. *Oncotarget* **2018**, *9*, 28042-28068.

[20] Guarra, F.; Marzo, T.; Ferraroni, M.; Papi, F.; Bazzicalupi, C.; Gratteri, P.; Pescitelli, G.; Messori, L.; Biver, T.; Gabbiani, C. Interaction of a gold (I) dicarbene anticancer drug with human telomeric DNA G-quadruplex: Solution and computationally aided X-ray diffraction analysis. *Dalton Trans.* **2018**, *47*, 16132-16138.

[21] Berggren, M.; Gallegos, A.; Gasdaska, J.R.; Gasdaska, P.Y.; Warneke, J.; Powis, G. Thioredoxin and thioredoxin reductase gene expression in human tumors and cell lines, and the effects of serum stimulation and hypoxia. *Anticancer Res.* **1996**, *16*, 3459-3466.

[22] Nakamura, H.; Bai, J.; Nishinaka, Y.; Ueda, S.; Sasada, T.; Ohshio, G.; Imamura, M.; Takabayashi, A.; Yamaoka, Y.; Yodoi, J. Expression of thioredoxin and glutaredoxin, redox-regulating proteins, in pancreatic cancer. *Cancer Detect. Prev.* **2000**, *24(1)*, 53-60.

[23] Arcau, J.; Andermark, V.; Rodrigues, M.; Giannicchi, I.; Peerez-Garcia, L.; Ott, I.; Rodríguez, L. Synthesis and biological activity of gold(I) N-heterocyclic carbene complexes with long aliphatic side chains. *Eur. J. Inorg. Chem.* **2014**, *2014(35)*, 6117-6125.

[24] Bertrand, B.; de Almeida, A.; van der Burgt, E. P. M.; Picquet, M.; Citta, A.; Folda, A.; Rigobello, M. P.; Le Gendre, P.; Bodio, E.; Casini, A. New gold(I) organometallic compounds with biological activity in cancer cells. *Eur. J. Inorg. Chem.* **2014**, *2014(27)*, 4532-4536.

[25] Roland, S.; Jolivalt, C.; Cresteil, T.; Eloy, L.; Bouhours, P.; Hequet, A.; Mansuy, V.; Vanucci, C., Paris, J.-M. Investigation of a series of silver–N-heterocyclic carbenes as antibacterial agents: Activity, synergistic effects, and cytotoxicity. *Chem. - A Eur. J.* **2011**, *17*, 1442-1446.

[26] Asekunowo, P.O.; Haque, R.A.; Razali, M.R.; Avicor, S.W.; Wajidi, M.F.F. Synthesis and characterization of nitrile functionalized silver (I)-N-heterocyclic carbene complexes: DNA binding, cleavage studies, antibacterial properties and mosquitocidal activity against the dengue vector, Aedes albopictus. *Eur. J. Med. Chem.* **2018**, *150*, 601-615.

[27] Johnson, N.A.; Southerland, M.R.; Youngs, W.J. Recent developments in the medicinal applications of silver-NHC complexes and imidazolium salts. *Molecules* **2017**, *22*, 1263:1-20.

[28] Garrison, J.C.; Youngs, W.J. Ag (I) N-heterocyclic carbene complexes: synthesis, structure, and application. *Chem. Rev.* **2005**, *105(11)*, 3978-4008.

[29] Kascatan-Nebioglu, A.; Panzner, M.J.; Tessier, C.A.; Cannon, C.L.; Youngs, W.J. N-Heterocyclic carbene-silver complexes: A new class of antibiotics. *Coord. Chem. Rev.* **2007**, *251*, 884-895.

[30] Guarra, F.; Busto, N.; Guerri, A.; Marchetti, L.; Marzo, T.; García, B.; Biver, T.; Gabbiani, C. Cytotoxic Ag (I) and Au (I) NHC-carbenes bind DNA and show TrxR inhibition. *J. Inorg. Biochem.* **2020**, *205*, 110998:1-11.

[31] Li, Y.; Liu, G.F.; Tan, C.P.; Ji, L.N.; Mao, Z.W. Antitumor properties and mechanisms of mitochondria-targeted Ag (I) and Au (I) complexes containing N-heterocyclic carbenes derived from cyclophanes. *Metallomics* **2014**, *6(8)*, 1460-1468.

[32] Karaca, O.; Scalcon, V.; Meier-Menches, S.M.; Bonsignore, R.; Brouwer, J.M.; Tonolo, F.; Folda, A.; Rigobello, M.P.; Kühn, F.E.; Casini, A. Characterization of hydrophilic gold (I) N-heterocyclic carbene (NHC) complexes as potent TrxR inhibitors using biochemical and mass spectrometric approaches. *Inorg. Chem.* **2017**, *56(22)*, 14237-14250.

[33] Pratesi, A.; Gabbiani, C.; Michelucci, E.; Ginanneschi, M.; Papini, A.M.; Rubbiani, R.; Ott, I.; Messori, L. Insights on the mechanism of thioredoxin reductase inhibition by gold N-heterocyclic carbene compounds using the synthetic linear selenocysteine containing C-terminal peptide hTrxR (488-499): An ESI-MS investigation. *J. Inorg. Biochem.* **2014**, *136*, 161-169.

[34] Visbal, R.; Fernández-Moreira, V.; Marzo, I; Laguna, A.; Gimeno, M.C. Cytotoxicity and biodistribution studies of luminescent Au (I) and Ag (I) N-heterocyclic carbenes. Searching for new biological targets. *Dalton Trans.* **2016**, *45*, 15026-15033.

[35] Citta, A.; Schuh, E.; Mohr, F.; Folda, A.; Massimino, M.L.; Bindoli, A.; Casini, A.; Rigobello, M.P. Fluorescent silver (I) and gold (I)–N-heterocyclic carbene complexes with cytotoxic properties: Mechanistic insights. *Metallomics* **2013**, *5(8)*, 1006-1015.

[36] Jakob, C.H.; Dominelli, B.; Schlagintweit, J.F.; Fischer, P.J.; Schuderer, F.; Reich, R.M.; Marques, F.; Correia, J.D.G.; Kühn, F.E. Improved antiproliferative activity and fluorescence of a dinuclear gold (I) bisimidazolylidene complex via anthracene-modification. *Chem. Asian J.* **2020**, *15(24)*, 4275-4279.

[37] Allison, S.J.; Sadiq, M.; Baronou, E.; Cooper, P.A.; Dunnill, C.; Georgopoulos, N.T.; Latif, A.; Shepherd, S.; Shnyder, S.D.; Stratford, I.J.; Wheelhouse, R.T. Preclinical anti-cancer activity and multiple mechanisms of action of a cationic silver complex bearing N-heterocyclic carbene ligands. *Cancer Lett.* **2017**, *403*, 98-107.

[38] Eloy, L.; Jarrousse, A.S.; Teyssot, M.L.; Gautier, A.; Morel, L.; Jolivalt, C.; Cresteil, T.; Roland, S. Anticancer activity of silver-N-heterocyclic carbene complexes: caspase-independent induction of apoptosis via mitochondrial Apoptosis-Inducing Factor (AIF). *ChemMedChem* **2012**, *7(5)*, 805-814.

[39] Touj, N.; Nasr, I.S.A.; Koko, W.S.; Khan, T.A.; Özdemir, I.; Yasar, S.; Mansour, L.; Alresheedi, F.; Hamdi, N. Anticancer, antimicrobial and antiparasitical activities of copper (I) complexes based on N-heterocyclic carbene (NHC) ligands bearing aryl substituents. *J. Coord. Chem.* **2020**, *73(20-22)*, 2889-2905.

[40] Teyssot, M.L.; Jarrousse, A.S.; Manin, M.; Chevry, A.; Roche, S.; Norre, F.; Beaudoin, C.; Morel, L.; Boyer, D.; Rachid Mahiou, R.; Gautier, A. Metal-NHC complexes: A survey of anti-cancer properties. *Dalton Trans.* **2009**, *35*, 6894-6902.

[41] Kagawa, T.F.; Geierstanger, B.H.; Wang, A.H.J.; Ho, P.S. Covalent modification of guanine bases in double-stranded DNA. *J. Biol. Chem.* **1991**, *266*, 20175-20184.

[42] Shobha Devi, C.; Thulasiram, B.; Aerva, R.R.; Nagababu, P. Recent advances in copper intercalators as anticancer agents. *J. Fluoresc.* **2018**, *28*, 1195-1205.

[43] Santini, C.; Pellei, M.; Papini, G.; Morresi, B.; Galassi, R.; Ricci, S.; Tisato, F.; Porchia, M.; Rigobello, M.P.; Gandin, V.; Marzano, C. In vitro antitumour activity of water soluble Cu (I), Ag (I) and Au (I) complexes supported by hydrophilic alkyl phosphine ligands. *J. Inorg. Biochem.* **2011**, *105(2)*, 232-240.

[44] Jacobsen, H.; Correa, A.; Poater, A.; Costabile, C.; Cavallo, L. Understanding the M (NHC)(NHC= N-heterocyclic carbene) bond. *Coord. Chem. Rev.* **2009**, *253(5-6)*, 687-703.

[45] Boehme, C.; Frenking, G. N-Heterocyclic carbene, silylene, and germylene complexes of MCl (M= Cu, Ag, Au). A theoretical study. *Organometallics* **1998**, *17(26)*, 5801-5809.

[46] Nemcsok, D.; Wichmann, K.; Frenking, G. The significance of π interactions in group 11 complexes with N-heterocyclic carbenes. *Organometallics* **2004**, *23(15)*, 3640-3646.

[47] Tonner, R.; Heydenrych, G.; Frenking, G. Bonding analysis of N-heterocyclic carbene tautomers and phosphine ligands in transition-metal complexes: A theoretical study. *Chem. Asian J.* **2007**, *2*, 1555-1567.

[48] Tolbatov, I.; Coletti, C.; Marrone, A.; Re, N. Insight into the substitution mechanism of antitumor Au (I) N-heterocyclic carbene complexes by cysteine and selenocysteine. *Inorg. Chem.* **2020**, *59(5)*, 3312-3320.

[49] Dos Santos, H.F.; Vieira, M.A.; Sánchez Delgado, G.Y.; Paschoal, D. Ligand exchange reaction of Au (I) RN-heterocyclic carbene complexes with cysteine. *J. Phys. Chem. A* **2016**, *120(14)*, 2250-2259.

[50] Tolbatov, I.; Coletti, C.; Marrone, A.; Re, N. Reactivity of gold (I) monocarbene complexes with protein targets: A theoretical study. *Int. J. Mol. Sci.* **2019**, *20(4)*, 820:1-15.

[51] Gaussian 09, Revision A.02, Gaussian, Inc., Wallingford CT, **2016**.

[52] Hay, P.J.; Wadt, W.R. Ab initio effective core potentials for molecular calculations. Potentials for K to Au including the outermost core orbitals. *J. Chem. Phys.* **1985**, *82*, 299-310.

[53] Francl, M.M.; Pietro, W.J.; Hehre, W.J.; Binkley, J.S.; Gordon, M.S.; DeFrees, D.J.; Pople, J.A. Self-consistent molecular orbital methods. XXIII. A polarization-type basis set for second-row elements. *J. Chem. Phys.* **1982**, *77*, 3654-3665.

[54] Gordon, M.S.; Binkley, J.S.; Pople, J.A.; Pietro, W.J.; Hehre, W.J. Self-consistent molecular-orbital methods. 22. Small split-valence basis sets for second-row elements. *J. Am. Chem. Soc.* **1982**, *104*, 2797-2803.

[55] Rassolov, V.A.; Ratner, M.A.; Pople, J.A.; Redfern, P.C.; Curtiss, L.A. 6-31G* basis set for third-row atoms. *J. Comput. Chem.* **2001**, *22*, 976-984.

[56] Roy, L.E.; Hay, P.J.; Martin, R.L. Revised Basis Sets for the LANL Effective Core Potentials. *J. Chem. Theory Comput.* **2008**, *4*, 1029-1031.

[57] McLean, A.D.; Chandler, G.S. Contracted Gaussian basis sets for molecular calculations. I. Second row atoms, Z=11-18. *J. Chem. Phys.* **1980**, *72*, 5639-5648.

[58] Tolbatov, I.; Marzo, T.; Cirri, D.; Gabbiani, C.; Coletti, C.; Marrone, A.; Paciotti, R.; Messori, L.; Re, N. Reactions of cisplatin and cis-[PtI2(NH3)2] with molecular models of relevant protein sidechains: A comparative analysis. *J. Inorg. Biochem.* **2020**, *111096*, 1-9.

[59] Tolbatov, I.; Re, N.; Coletti, C.; Marrone, A. Determinants of the Lead (II) affinity in pbrR protein: A computational study. *Inorg. Chem.* **2019**, *59(1)*, 790-800.

[60] Paciotti, R.; Tolbatov, I.; Graziani, V.; Marrone, A.; Re, N.; Coletti, C. Insights on the activity of platinum-based anticancer complexes through computational methods. In: AIP conference proceedings (2018, Vol. 2040, No. 1, p. 020019). AIP Publishing LLC.

[61] Tolbatov, I.; Marrone, A. Molecular dynamics simulation of the Pb(II) coordination in biological media via cationic dummy atom model. *Theor. Chem. Acc.* **2021**, *140(20)*, 1-12.

[62] Paciotti, R.; Tolbatov, I.; Marrone, A.; Storchi, L.; Re, N.; Coletti, C. Computational investigations of bioinorganic complexes: The case of calcium, gold and platinum ions. In AIP Conference Proceedings (2019, Vol. 2186, No. 1, p. 030011). AIP Publishing LLC. https://doi.org/10.1063/1.5137922

[63] Nassar, M. Y.; El-Shwiniy, W. H.; El-Desoky, S. I. Synthesis of Pd(II), Ag(I), Pt(IV), and Hg(II) complexes with nifuroxazide, their structure, DFT modeling, and antimicrobial and anticancer activity. *Rus. J. Gen. Chem.* **2018**, *88(3)*, 573-579.

[64] Usman, M.; Arjmand, F.; Khan, R.A.; Alsalme, A.; Ahmad, M.; Tabassum, S. Biological evaluation of dinuclear copper complex/dichloroacetic acid cocrystal against human breast cancer: Design, synthesis, characterization, DFT studies and cytotoxicity assays. *RSC Adv.* **2017**, *7(76)*, 47920-47932.

[65] Tolbatov, I.; Re, N.; Coletti, C.; Marrone, A. An insight on the gold (I) affinity of golB protein via multilevel computational approaches. *Inorg. Chem.* **2019**, *58(16)*, 11091-11099.

[66] Tolbatov, I.; Cirri, D.; Marchetti, L.; Marrone, A.; Coletti, C.; Re, N.; La Mendola, D.; Messori, L.; Marzo, T.; Gabbiani, C.; Pratesi, A. Mechanistic insights Into the anticancer properties of the auranofin analog $Au(PEt_3)I$: A theoretical and experimental study. *Front. Chem.* **2020**, *8*, 812:1-13.

[67] Barresi, E.; Tolbatov, I.; Pratesi, A.; Notarstefano, V.; Baglini, E.; Daniele, S.; Taliani, S.; Re, N.; Giorgini, E.; Martini, C.; Da Settimo, F.; Marzo, T.; La Mendola, D. A mixed-valence diruthenium (II, III) complex endowed with high stability: From experimental evidence to theoretical interpretation. *Dalton Trans.* **2020**, *49(41)*, 14520-14527.

[68] Todisco, S.; Latronico, M.; Gallo, V.; Re, N.; Marrone, A.; Tolbatov, I.; Mastrorilli, P. Double addition of phenylacetylene onto the mixed bridge phosphinito–phosphanido Pt (I) complex [(PHCy 2) Pt (μ-PCy 2){κ 2 P, O-μ-P (O) Cy 2} Pt (PHCy 2)](Pt–Pt). *Dalton Trans.* **2020**, *49(20)*, 6776-6789.

[69] Chai, J.D.; Head-Gordon, M. Systematic optimization of long-range corrected hybrid density functionals. *J. Chem. Phys.* **2008**, *128(8)*, 084106:1-15.

[70] Tolbatov, I.; Coletti, C.; Marrone, A.; Re, N. Reactivity of arsenoplatin complex versus water and thiocyanate: A DFT benchmark study. *Theor. Chem. Acc.* **2020**, *139(12)*, 1-11.

[71] Dohm, S.; Hansen, A.; Steinmetz, M.; Grimme, S.; Checinski, M.P. Comprehensive thermochemical benchmark set of realistic closed-shell metal organic reactions. *J. Chem. Theory Comput.* **2018**, *15*, 2596-2608.

[72] Cossi, M.; Rega, N.; Scalmani, G.; Barone, V. Energies, structures, and electronic properties of molecules in solution with the C-PCM solvation model. *J. Comput. Chem.* **2003**, *24(6)*, 669-681.

[73] Chen, J.; Shao, Y.; Ho, J. Are explicit solvent models more accurate than implicit solvent models? A case study on the Menschutkin reaction. *J. Phys. Chem. A* **2019**, *123(26)*, 5580-5589.

[74] Baker, M.V.; Barnard, P.J.; Berners-Price, S.J.; Brayshaw, S.K.; Hickey, J.L.; Skelton, B.W.; White, A.H. Cationic, linear Au(I) N-heterocyclic carbene complexes: Synthesis, structure and anti-mitochondrial activity. *Dalton Trans.* **2006**, *30*, 3708-3715.

[75] Kolychev, E.L.; Portnyagin, I.A.; Shuntikov, V.V.; Khrustalev, V.N.; Nechaev, M.S. Six- and seven-membered ring carbenes: Rational synthesis of amidinium salts, generation of carbenes, synthesis of Ag (I) and Cu (I) complexes. *J. Organomet. Chem.* **2009**, *694(15)*, 2454-2462.

[76] Chen, W.; Liu, F. Synthesis and characterization of oligomeric and polymeric silver-imidazol-2-ylidene iodide complexes. *J. Organomet. Chem.* **2003**, *673(1-2)*, 5-12.

[77] Ibrahim, H.; Gibard, C.; Hesling, C.; Guillot, R.; Morel, L.; Gautier, A.; Cisnetti, F. 'Auto-click' functionalization for diversified copper (I) and gold (I) NHCs. *Dalton Trans.* **2014**, *43(19)*, 6981-6989.

[78] Graziani, V.; Marrone, A.; Re, N.; Coletti, C.; Platts, J.A.; Casini, A. A multilevel theoretical study to disclose the binding mechanisms of gold (III) bipyridyl compounds as selective aquaglyceroporin inhibitors. *Chem. Eur. J.* **2017**, *23(55)*, 13802-13813.

[79] Canal, J.P.; Ramnial, T.; Clyburne, J.A.C. A carbene transfer agent. In: Experiments in Green and Sustainable Chemistry, ed. H. W. Roesky and D. K. Kennepohl, Wiley-VCH, Weinheim, 2009, p. 25ff

[80] Zhang, J.; Zhang, B.; Li, X.; Han, X.; Liu, R.; Fang, J. Small molecule inhibitors of mammalian thioredoxin reductase as potential anticancer agents: an update. *Med. Res. Rev.* **2019**, *39*, 5-39.

[81] De Santis, M.; Rampino, S.; Quiney, H.M.; Belpassi, L.; Storchi, L. Charge-Displacement Analysis via Natural Orbitals for Chemical Valence in the Four-Component Relativistic Framework. *J. Chem. Theory Comput*. **2018**, *14***,** 1286−1296

[82] De Santis, M.; Rampino, S.; Storchi, L.; Belpassi, L.; Tarantelli, F. The Chemical Bond and s−d Hybridization in Coinage Metal(I) Cyanides, *Inorg. Chem*. **2019**, *58*, 11716−11729

For Table of Contents Only

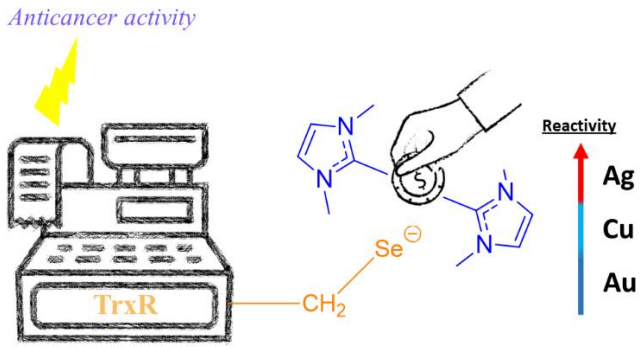

Reactions of antitumor M(I)-bis-N-heterocyclic carbene complexes, M=Cu, Ag, and Au, with their potential protein binding sites, cysteine and selenocysteine, were computationally investigated considering several pathways to account for environmental influence through the ionization state of the aminoacidic side chains and the possible assistance of proton transfer to the leaving carbene moiety. Environment is shown to play a crucial role in the feasibility of the reaction and the complexes exhibit thermodynamic and kinetic preference in the order Ag(I)>Cu(I)>Au(I).